ORIGINAL ARTICLE

INTERNATIONAL JOURNAL OF RESEARCH IN PHARMACEUTICAL SCIENCES

Published by JK Welfare & Pharmascope Foundation Journal Home Page: www.pharmascope.org/ijrps

In situ gel loaded with curcumin-based fluvastatin nanostructured carrier effective against squamous tongue carcinoma

Amal M. Sindi*

Oral Diagnostic Science Department, Faculty of Dentistry, King Abdulaziz University, Jeddah, Saudi Arabia

Article History:

Received on: 04.04.2019
Revised on: 18.07.2019
Accepted on: 22.07.2019

Keywords:

Fluvastatin,
Curcumin,
Nanostructured Lipid Carriers,
In-situ gel,
HCS 3 cell line,
Tongue Carcinoma

ABSTRACT

The aim of the study was to devise a novel Fluvastatin (FT) based curcumin (CR) nanostructured lipid carrier (NLC) loaded into an in situ gelling system (ISG) for localized and prolonged chemotherapy in the treatment of aggressive tongue carcinoma. FT-CR NLC was prepared using the solvent evaporation method, characterized, and optimized. FT-CR NLC was loaded in a Poloxamer 407 and polyvinyl alcohol-based ISG, further characterized and evaluated. The percentage of cellular viability and caspase-3 enzyme levels were evaluated for the optimized FT-CRNLC, and loaded ISG formulations were applied to HCS-3 cancer cell lines. Stability studies were performed. The optimized FT-CR NLC was spherical with an indicated particle size of 107 ± 4.5 nm, a polydispersity index of 0.38 ± 0.6, surface charge of -31.1 ± 1.8 mV, and entrapment efficiency of 98.4% ± 0.81%. The optimized ISG had an optimum sol-gel transition temperature. The FT IC50 was decreased by half for FT-CR NLC–loaded ISG in comparison to plain FT and FT-CR NLC. The studies indicated that CR's synergistic anti-oxidant effect in the FT NLC formulation led to a higher inhibition against HCS-3 cancer cell lines. FT-CR NLC–loaded ISG had a prolonged release that can be significant in localized therapy as an alternative to surgery, especially in the treatment of aggressive tongue squamous cell carcinoma.

*Corresponding Author

Name: Amal M. Sindi
Phone: 00966561682377
Email: amalsindi2020@gmail.com

ISSN: 0975-7538

DOI: https://doi.org/10.26452/ijrps.v10i3.1456

Production and Hosted by

Pharmascope.org

INTRODUCTION

Oral cancer is one of the most common forms of cancer in humans, arising from squamous cells and affecting the oral cavity and pharynx. With poor treatment and prognosis, male smokers are at higher risk for oral cancer and account for 50% of mortalities across the globe (Warnakulasuriya, 2009). Improvement in average survival rates is minimal due to drawbacks in standard chemotherapy, such as indigent drug specificity, unwanted effects, and over treatment. Surgical removal remains as the final treatment option (Hirano *et al.*, 1992). Statins such as 3-hydroxy-3-methylglutaryl coenzyme A (HMGA CoA) reductase inhibitors are employed in the treatment of hypercholesterolemia (Doktorovova and Souto, 2009). In addition to cholesterol reduction, statins are reported to exhibit direct anti-inflammatory and antithrombotic activity and are now recognized for their pleiotropic cellular outcomes, inhibiting metastasis and regulating the cell cycle in tumor cells. For example, fluvastatin (FT) is reported to inhibit the formation and further growth of liver metastases in pancreatic cancer cells (Taylor *et al.*, 2011). FT, when used alone, can effectively induce apoptosis and can stabilize squamous cell oral or tongue carcinomas (Bocci *et al.*, 2005).

Administration of statins, along with a phytocompound that has antioxidant properties, has yielded better results. For example, simvastatin combined with alpha-lipoic acid exhibited enhanced toxicity against breast carcinoma cell lines (Fujiwara *et al.*, 2008). Effective localized delivery of FT along with a natural anti-oxidant using nanocarriers needs to be explored.

Curcumin (CR) (diferuloylmethane) is the main constituent of turmeric, a spice derived from the rhizome of the plant *Curcuma longa*. By virtue of their chemical structure, curcuminoids that have two methoxylated phenols in stable enol form exhibit potential antioxidant activity (Fahmy and Al-jaeid, 2016). It is reported that CR, in response to oxidative stress, downregulates iNOS activity in macrophages, thereby reducing concentrations of reactive oxygen species (ROS) (Masuda *et al.*, 1999). CR has been shown to inhibit Phase I enzymes and induce Phase II enzymes involved in carcinogenic metabolites. The inhibitory effect of CR on carcinogenesis has been reported in tumor animal models, including intestinal, oral, and mammary carcinomas (Jayaprakasha *et al.*, 2006). The synergistic effect of CR combined with FT to inhibit oral squamous cell carcinoma has not been explored previously and may be a breakthrough in treatment. Nanostructured lipid carriers (NLCs) are versatile, bio compatible nanosystems formed from the mixture of solid and liquid lipids and have an unstructured matrix due to their various components. NLCs are recognized for their high drug-loading capacity due to their unequal crystal structure and even for avoiding drug expulsion during storage (Huang *et al.*, 1994). NLCs provide greater penetration into cells, extended circulation in vivo, greater stability, and less susceptibility to gelation, which can facilitate their incorporation into suitable systems (Radtke and Müller, 2001) for localized oral delivery, especially in the treatment of tongue carcinoma. In situ gel (ISG) forming systems (injectable) are fluids that rapidly undergo gelation/solidification in response to several external stimuli, such as temperature, solvent (Ruel-Gariépy and Leroux, 2004). These systems are free-flowing at room temperature but solidify after injection into the body. Cellulose derivatives, polyethylene oxide-b-propylene oxide-b-ethylene oxide (Poloxamer)/copolymers and poly(ethylene oxide)/(D, L-lactic acid-co-glycolic acid) copolymers transform into gel in response to external temperature changes (Ito *et al.*, 2007). Poloxamer 407 (P 407) (high concentration) aqueous solutions with polyvinyl alcohol (PVA) tend to form thermoresponsive gels as in situ gel (Taheri *et al.*, 2011).

In order to over-come physiochemical barriers of FT, NLC can be beneficial and to evaluate its repurpose use in the chemotherapy of tongue carcinoma loaded into the in-situ gelling system for localized delivery would be essential. Therefore, the present study aims to formulate FT NLC using the solvent evaporation method with CR as an antioxidant loaded in Poloxamer based in situ gel for prolonged-release and to evaluate its effectiveness against HSC-3 tongue carcinoma cell lines.

MATERIALS AND METHODS

FT was a gift sample from Bayer, Germany. Egg lecithin, isopropyl myristate, and D-tocopherol polyethylene glycol succinate (TPGS) were obtained from Acros Organics, USA. Stearic acid, PVA (Mw: 9000–10,000; 80% hydrolyzed) and Tween 80 were purchased from Sigma Aldrich, USA. HSC-3 cell lines were a gift from the Department of Pharmacology, King Abdulaziz University, Saudi Arabia. All other solvents, chemicals, and reagents used were of analytical grade.

Preparation of FT-CR NLC

NLC formulation was optimized by varying formulation parameters such as phospholipid (egg lecithin), surfactant (Tween 80), and emulsifier (TPGS). A series of nine formulations were prepared (Table 1) to understand the effect of components in terms of size, charge, and percentage entrapment efficiency (% EE). NLC-loaded FT (5%) and CR (0.5%) were prepared using the solvent evaporation method (Uner, 2006). Stearic acid and isopropyl myristate were used in a 4:1 weight ratio. Equivalent weights of FT, CR, phospholipid, and emulsifier were dissolved in chloroform at different ratios. The organic phase was slowly added dropwise to the aqueous phase consisting of Tween 80 and homogenized (UltraTurrax T25, IKA, Germany) at 10,000 rpm for 15 min. The emulsion was probe sonicated (Vibra cell, Sonics, USA) at 45% amplitude for 15 min. The formulation was left for stirring for 3 h to remove the residual organic solvents and, finally, lyophilized and stored in a tight container.

Preparation of FT-CR NLC–loaded ISG

Optimization and preparation of P 407 solutions was performed using a previously reported cold method (Chen *et al.*, 2016). An equivalent amount of prepared FT-CR NLC was added, and the gels were characterized for their visual appearance, pH, and gelation time.

Characterization of FT-CR NLC formulation

Determination of particle size and particle size distribution (PDI)

Table 1: Different components and wt ratios selected for optimization of FT NLC

Formulation	Egg Lecithin (%)	Tween 80 (%)	TPGS (%)
F1	15	0	0
F2	0	15	0
F3	0	0	15
F4	10	10	0
F5	10	0	10
F6	0	10	10
F7	20	10	0
F8	15	20	0
F9	0	15	10

Approximately 1 mg of FT-CR NLC was dispersed in 3 mL of Millipore water. All measurements were performed in triplicate (n = 3) at 25°C at a 90° scattering angle using a Zetasizer NanoZS 90 (Malvern Instruments, UK).

Determination of zeta potential

Approximately 1 mg of FT-CR NLC was diluted in a 1:10 ratio using deionized distilled water. The electrophoretic mobility was measured in zeta cell (disposable) using a Zetasizer NanoZS 90. All samples were analyzed in triplicate (n = 3).

Determination of drug % EE

Accurately weighed FT-CR NLC was dissolved in methanol (3 mL) and ultra-centrifuged (Thermo Scientific Sorvall, Pittsburgh, PA, USA) at 11,000 rpm for 44 min to separate the aqueous and lipid phase. The obtained supernatant was diluted with the mobile phase and quantified at λ_{max} 304 nm using a slight modification of a previously reported high-performance liquid chromatography (HPLC) method (Nakashima *et al.*, 2001).

% EE = (initial amount of drug added − free drug / initial amount of drug added) × 100 (1)

Determination of surface morphology

The dry NLC was evenly mounted on the metallic stub and sputter-coated with gold. The imaging was performed using Scanning electron microscopy (Carl Zeiss Meditec AG, Jena, Germany) at an accelerating voltage of 15 to 18 kV. The images were recorded and saved.

Stability studies

The optimized formulation was evaluated for a period of 3 months for its stability at different temperature and humidity conditions as per ICH Q1 AR2 guidelines. Parameters such as size, surface charge, and % EE were evaluated.

FT-CR NLC–loaded ISG characterization

Determination of gelation temperature by visual examination

Two glass tubes (10 mL) were taken, each containing 1 g of sample and 1 mL of water. A thermometer was inserted into the tubes, and both tubes were placed into a water bath. The temperature of the water bath was gradually increased, and the point at which the sample flow stopped upon inverting was recorded (T1). Conversely, the temperature was gradually decreased, and the gel flow time was recorded (T2). The critical gelation temperature of prepared FT-CR NLC–loaded ISG was determined by calculating the average of both temperatures (T1 and T2) (Jeong *et al.*, 2000).

In vitro drug release studies

A membraneless dissolution model was adopted to determine FT release from the FT-CR NLC–loaded ISG and plain FT-CR–loaded ISG. One gram of cold formulation solution was put into a glass tube and placed in the 37°C water bath. Once gelation was attained, 500 μL of phosphate buffer solution (pH 7.2; pre-equilibrated at 37°C) was dropped on the formulation surface. At predetermined time points (0, 2, 8, 24, 48, 72, 96, 144, 168, and 192 h) the complete medium was aliquotted and immediately replaced with fresh release medium (Zhang, 2002). The samples were quantified at λ_{max} 304 nm by the previously reported HPLC method in triplicate.

In vitro cell viability assay

The prepared formulations of FT-CR NLC, FT-CR NLC–loaded ISG, and plain FT were evaluated for their in vitro cytotoxicity against HCS-3 cells by the 3-[4,5-dimethylthiazol-2-yl]-2,5-diphenyltetrazolium bromide (MTT) method. Briefly, exponentially growing HCS-3 cells at a cell density of 5×10^4 cells/mL were trypsinized using 0.25% trypsin-EDTA and seeded in a 96-well plate at about 2500-5000 cells/well. After 24 h, the medium was replaced

with fresh Dulbecco's Modified Eagle Medium (DMEM). The cells were treated with 5-fluorouracil as control, plain FT, FT-CR NLC, and FT-CR NLC–loaded ISG at a concentration of 10 to 50 μg/mL and incubated for 72 h. Then 0.1 mL of DMEM having 0.2 mg/mL MTT was added and incubated for 2-3 h. The DMEM was removed, and 100 uL of DMSO was added to dissolve the formazan formed. The absorbance was measured at 540 nm using a microplate reader (Biotek Synergy, USA). IC 50 was determined using a dose-responsive curve (Chien *et al.*, 2012).

Caspase-3 enzyme assay

Plain FT, FT-CR NLC, and FT-CR NLC–loaded ISG were tested. The cells were cultured in RPMI 1640, consisting of 10 % fetal bovine serum at 37°C, tested for caspase-3, and further lysed using cell extraction buffer. The collected lysate was diluted in the standard diluent buffer as per the assay range for human active caspase-3 traces. Furthermore, the cells were plated at 1.3-1.9 × 10,000 cells/well in DMEM (100 μL). Twenty-four hours before the caspase-3 assay, each sample was inoculated in a 96-well plate (Lin, 2007). The assay was carried out using spectrophotometry at 450 nm, as per the kit instructions (USCN Life Science Inc., China).

Statistical analysis

One-way analysis of variance (GraphPad Prism v5.01, GraphPad Software, San Diego, California) was used to analyze data for multiple comparisons. The level of significance was set at $p < 0.05$.

RESULTS AND DISCUSSION

Preparation of FT-CR NLC

Components such as stearic acid and isopropyl myristate were used as the solid and liquid matrix for stable formation of NLC.

Particle size, zeta potential, and PDI measurements

Different components used in the preparation of FT-CR NLC revealed their effect on the quality of NLC formed. Shown in Table 1, the concentration of components chosen for F1, F2, F3, and the NLC size gradually increased, with more than -21 mV surface charge, which indicates poor stability of the NLC. In contrast, F4 and F5 were smaller (<120 nm) in comparison to other formulations at 92.6 ± 2.5 and 107 ± 4.5 nm, respectively. Overall, all formulations have indicated values from -9.3 ± 0.4 mV to -35.1 ± 0.2 mV, indicating F4 as more stable in the aqueous dispersion environment in comparison to the other formulations. The PDI of all formulations ranged from 0.23 ± 0.8 to 0.68 ± 0.6; a PDI value <0.5 is regarded as having better stability. In terms of structure size, PDI, and charge, formulation F4 was best and hence was selected as the optimized formulation. The mean zeta potential, PDI, and particle size, along with % EE, are depicted in Table 2.

Determination of % EE

In Table 2 it is evident that when egg lecithin and TPGS were used as an emulsifier matrix (F5), the FT loading was approximately 1.5-fold higher than in F4 (egg lecithin and Tween 80) and F6 (Tween 80 and TPGS). The formulation consisting of egg lecithin and TPGS had a better FT % EE ($p < 0.05$) in comparison to formulations having egg lecithin and Tween 80. TPGS systems alone or with Tween 80 ($p < 0.05$) even had a higher % EE.

Surface morphology studies

The optimized FT-CR NLC F5 was spherical with smooth surfaces that are distinct and without aggregation (Figure 1).

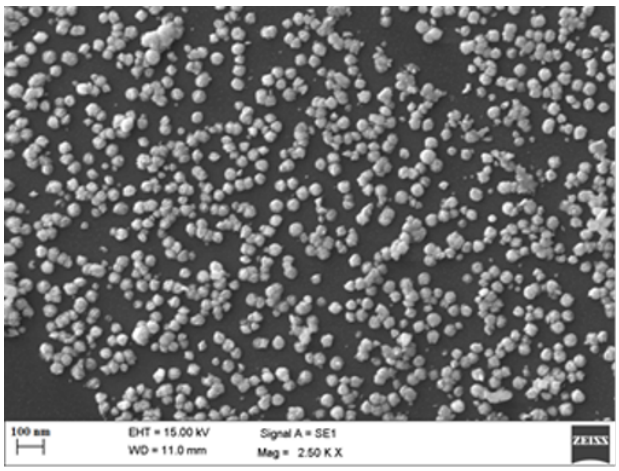

Figure 1: SEM image of optimized F5 formulation

Stability studies

Significant differences in particle size, zeta potential, and % EE were observed after 3 months, indicating that NLC has long-term stability. (Table 3)

Optimization of ISG and loading of FT-CR NLC

Different concentrations of P 407 and PVA were used to formulate the optimized ISG for FT-CR NLC loading indicated in Table 4. The optimized ISG was developed by using a minimal concentration of P 407 (14%) with the addition of PVA. The final FT-CR NLC–loaded ISG formulation was transparent with good rheological properties.[30]

Visual measurement of gelation temperature:

Composition B (14 % P 407 and 10 % PVA) from Table 5 had a higher critical gel temperature at 27.2 °C

Table 2: Characterization of NLC for particle size, zeta potential, and % EE

Formulation	Particle Size (nm)	Zeta Potential (mV)	PDI	% EE
F1	156 ± 2.4	- 22.3 ± 0.2	0.48 ± 0.5	10.2 ± 0.21
F2	174 ± 1.5	-24.3 ± 1.5	0.54 ± 0.1	3.7 ± 0.35
F3	256 ± 0.4	-26.1 ± 3.1	0.38 ± 0.4	15.2 ± 0.47
F4	92.6 ± 2.5	- 35.1 ± 0.2	0.23 ± 0.8	92.1 ± 0.65
F5	107 ± 4.5	-31.1 ± 1.8	0.38 ± 0.6	98.4 ± 0.81
F6	332 ± 3.5	-9.3 ± 0.4	0.36 ± 0.2	58.3 ± 0.66
F7	199 ± 0.2	-15.6 ±0.7	0.44 ± 0.9	31.5 ± 0.84
F8	184 ± 3.2	-22.2 ± 0.6	0.52 ± 0.5	76.2 ± 0.54
F9	212 ± 1.3	-12.1 ± 2.1	0.32 ± 0.3	61.2 ± 0.21

Table 3: Results of stability studies

Optimized Formula (F5)	Temp. °C	Particle size (nm)		PV	Zeta potential (mV)		PV	Entrapment efficiency (%)		PV*
		0 month	3 month		0 month	3 month		0 month	3 month	
FT-CR NLC	4	107 ± 4.5	108 ± 2.3	0.93	-31.1 ± 1.8	-30.2 ± 2.5	0.9	98.4 ± 0.81	96.5 ± 0.21	1.9
	24	107 ± 4.5	109 ± 1.2	1.87	-31.1 ± 1.8	-29.2 ± 2.5	1.9	98.4 ± 0.81	97.2 ± 0.15	1.2

*PV: Percent Variation

Table 4: Polymer composition of blank ISG system

Polymer	Composition		
	A (%)	B (%)	C (%)
Poloxamer 407	14	14	10
Polyvinyl alcohol	14	10	14

and was selected for further evaluations.

Table 5: Critical gelation temperature of blank ISG

Composition	T1 (°C)	T2 (°C)	Average (°C)
A	20.1	19.3	19.7
B	28.1	26.3	27.2
C	27.5	25	26.2

In vitro release studies

Figure 2. Indicates the comparison of the cumulative percentage of FT released from plain FT, optimized FT-CR NLC, and FT-CR NLC–loaded ISG as a function of time. At 24 h an initial burst release was observed from FT-CR NLC in comparison to FT-CR NLC–loaded ISG. At the first 24 h, about 65.68 ± 1.2 cumulative percentages FT was released from FT-CR NLC, which was reduced to 35.3% ± 2.3% for FT-CR NLC–loaded ISG. The drug release from plain FT was very low due to solubility issues, whereas FT from FT-CR NLC and FT-CR NLC–loaded ISG was concentration dependent and continuous for the next few days. The release of FT from FT-CR NLC–loaded ISG was slower to plateau at up to 96 h but was continuous up to 14 days. However, there was 92.3% ± 2.4% cumulative release of FT-CR NLC at 144 h, in comparison to FT-CR NLC–loaded ISG, which had a steady state of 50.2% ± 1.7%.

In vitro cell viability assay

Five treatments (plain FT, FT NLC, FT-CR NLC, FT-CR NLC–loaded ISG, and 5 fluorouracil as a control) at 10 to 50 μg/mL were applied to HSC-3 cell lines. Figure 3 shows that all treatments reduced cell viability in a dose-dependent way. The IC50 values of the treatments were as follows: plain FT, 74.5 ± 2.1 μM; FT NLC, 21.6 ± 4.2 μM; FT-CR NLC, 19.4 ± 4.2 μM; FT-CR NLC–loaded ISG, 16.6 ± 1.6 μM; and 5 flu-

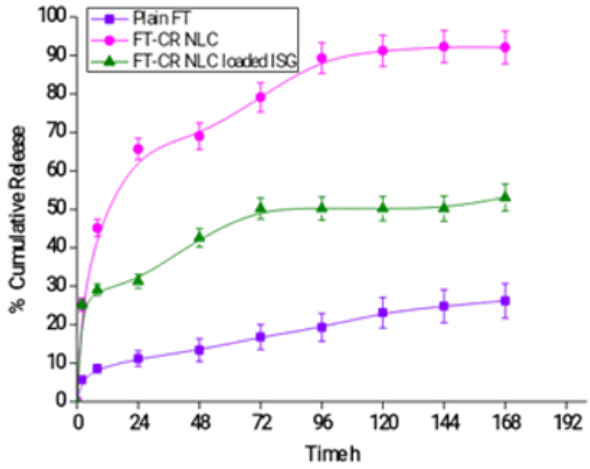

Figure 2: Comparison of in vitro release profiles of plain, NLC, and NLC-loaded ISG formulations

orouracil, 2.6 ± 0.4 μM. The observed IC50 for FT-CR NLC was lower than that of FT NLC, indicating the effect of CR in yielding higher cytotoxicity against HSC-3 cells.

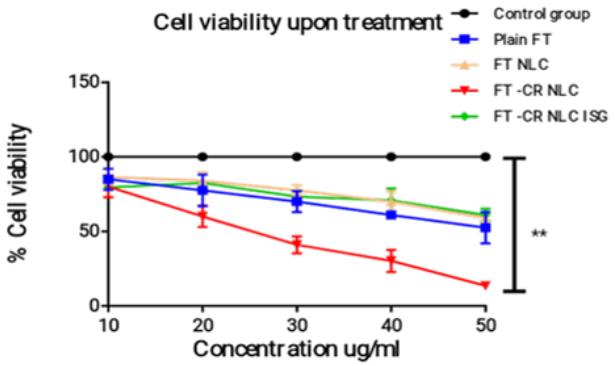

Figure 3: HSC 3 cell viability evaluated by MTT assay after 72 h treatment with different formulations. For the control group, cell viability was normalized to 100. The values represent the mean ± SD of three independent experiments (n = 9).

Caspase-3 Enzyme Assay

In all treatment formulations of the study, a significant amount of caspase-3 was detected in HCS-3 cells as depicted in Figure 4.

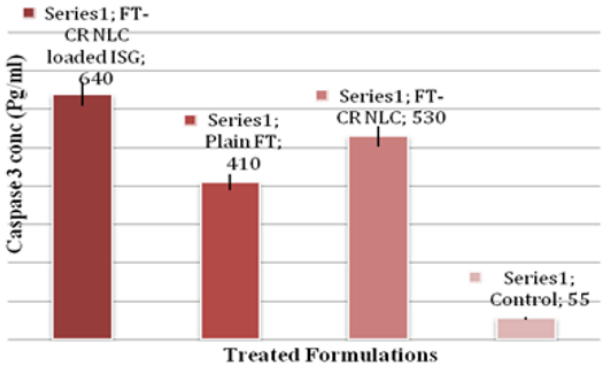

Figure 4: Caspase-3 enzyme concentrations in HCS-3 cells treated with different formulations and control(solvent-free); data are presented as the mean ± SD (n = 6).

Currently, there are limited therapeutic strategies for the treatment of tongue carcinoma. Drug repurposing and advances in formulation techniques are very promising and are being evaluated for providing long term effectiveness. NLC stand out for their high loading and better transfection efficiencies treating various carcinomas and ISG for providing localisation and prolonged release of the drug. In-depth evaluation of formulations using in-vitro models would enable the innovator product to be clinically useful. The selection of phospholipid-like egg lecithin was crucial in determining the structure and stability of NLC. Optimization of the phospholipid concentration had a significant effect on the size of the NLC, as reported earlier (Chen *et al.*, 2010). Tween 80 was selected as a surfactant and can provide cohesive forces between non-aqueous and aqueous phases and thus minimize droplet contact, enhancing the emulsion stability as a complement to TPGS (Teeranachaideekul *et al.*, 2007). TPGS was selected because of its better emulsifier properties and enabled uniform solubility of FT and even CR. CR (0.5% concentration) was fixed based on the previously reported data for optimum free radical scavenging capacity (Chen-Yu *et al.*, 2012).

For F1, F2 and F3, the % EE was almost negligible because they easily emerge and floccule when TPGS, egg lecithin, and Tween 80 were used as separate emulsifiers. Although the solubility and physiochemical properties of FT and CR play an important role, the nature of the surfactant has a significant role in FT-CR localization within the lipid carrier. Emulsifiers can hold back the FT-CR by reducing their leakage from the oil droplets, aiding in better EE within the NLC. The head (hydrophilic) portion of tocopherol succinate and bulky alkyl tail (lipophilic) from polyethylene glycol of TPGS has a bulky, large surface area that effectively protects against partition and diffusion of FT-CR from the polymer interface to the external phase (Gabal *et al.*, 2014). Therefore, the % EE of FT-CR is significantly improved in the NLC. The stability of optimized FT-CR NLC formulation could be attributed to the fact that FT was completely dissolved in the lipid matrix. (Zhang *et al.*, 2010) Furthermore, Tween 80 and TPGS reduced the electrostatic repulsion between particles, leading to better stabilization and forming a layered

structure around the particles (Zhou, 2012; Yuan *et al.*, 2012).

The release of FT from the formulation was concentration dependent, indicating first-order kinetics. In comparison to FT-CR NLC, which was biphasic, the release of FT from P 407–based ISG occurred due to the diffusion of FT through water channels within the gel matrix and FT (Madane and Mahajan, 2016; Bhowmik *et al.*, 2013; Jabarian *et al.*, 2013). If the disintegration of the NLC lipid matrix was a criterion for fast release of FT from NLC, both NLC and NLC-loaded ISG would have exhibited the same release profile. The initial burst release of FT from NLC at 24 h was solely due to FT at the surface of NLC, which allowed greater diffusion of water through the liquid matrix and faster release of FT. FT-CR NLC showed dose-dependent cell viability compared to the control group. The cell viability showed saturation at 40 μg/mL. Hence, FT-CR NLC showed better cytotoxic activity compared to all other treatments. FT exhibited high toxicity through inhibition of 3-hydroxy-3-methylglutaryl coenzyme A reductase, which in turn decreases mevalonate levels, thereby reducing dolichol, cholesterol, geranylgeranyl pyrophosphate, and farnesyl pyrophosphate type isoprenoid intermediates. These intermediates are connected to vital proteins, including Rho and GTP-restricting Ras (Tricarico *et al.*, 2015; Hooff *et al.*, 2010). Isoprenylation of the Rho and Ras proteins is directly inhibited by FT (Wheeler, 2006). The difference in the IC50 of FT-CR and FT-CR NLC was significant due to high affinity to the Pgp efflux transporter and higher penetration, cellular uptake micropinocytosis, (Cho *et al.*, 2005) and endocytosis in comparison to FT-CR NLC–loaded ISG, which had slower overall release of FT within the 72-h incubation period (Visvikis *et al.*, 2008; Han *et al.*, 1999). CR is a potent antioxidant known for its ability to generate ROS at different concentrations across different cancer cells. The previous reports revealed that a CR concentration of 5-10 mM starts cleavage of caspase-3 and down-regulation of Bcl-XL and Mcl-1 (anti-apoptotic factors). CR was even reported to reduce carcinogenesis (Rashmi, 2004) and was found to activate the mitochondrial-based death pathway in MIA PaCa-2 (human pancreatic carcinoma cell line) via down-regulation of nuclear factor-kappa B (NF-kB), further activating cytochrome-3 and finally causing mitochondrial death (Sun *et al.*, 2008). At 48 h of exposure, a 10 mmol/L amount of CR promoted trafficking of AIF, Endo G, ATF-4, and GADD153 distributions from the mitochondria in SCC-4 cells, leading to cell apoptosis through caspase-independent mitochondrial and ER stress signaling pathways. This result can be beneficiary in the treatment of oral squamous cell carcinoma (Ip *et al.*, 2011). Regulation of apoptosis depends upon the activation of caspases (cysteinyl aspartate-specific proteinases). The intensity of cytotoxicity and the amount of drug uptake at the cellular level are highly correlated. Nanosized FT-CR NLC (100-150 nm) can easily penetrate into the leaky neovasculature of cancer tissue (Rashmi, 2004). The present study illustrates that this novel strategy can be an alternative to surgery and can be extended to sustained release of other statins, especially in the treatment of aggressive squamous cell tongue carcinoma.

CONCLUSIONS

In the present study, FT-CR NLC was successfully prepared using the solvent evaporation technique, and the optimized formulation (F5) was loaded in a P 407 (14%)–PVA-based ISG system having an average gelation temperature of 27°C. No significant difference was observed between optimized FT-CR NLC and the loaded ISG in terms of morphology, % EE, or size, indicating good stability at elevated temperature. The study confirmed the synergetic effect of CR on FT cytotoxicity against HSC-3 tongue carcinoma cells. The particle size, charge, and % EE of F5 indicated the impact on cytotoxicity. Caspase-3 enzyme assays corroborated that the incidence of apoptosis caused by FT-CR NLC ISG was greater than that with other treatments. Incorporating the FT-CR NLC into gel offers a suitable sustained delivery of FT from the biodegradable in situ gel matrix.

REFERENCES

Bhowmik, M., Kumari, P., Sarkar, G., Bain, M. K., Bhowmick, B., Mollick, M. M. R., Chattopadhyay, D. 2013. Effect of xanthan gum and guar gum on in situ gelling ophthalmic drug delivery system based on poloxamer-407. International Journal of Biological Macromolecules, 62:117–123.

Bocci, G., Fioravanti, A., Orlandi, P., Bernardini, N., Collecchi, P., Tacca, M. D., Danesi, R. 2005. Fluvastatin synergistically enhances the antiproliferative effect of gemcitabine in human pancreatic cancer MIAPaCa-2 cells. British Journal of Cancer, 93(3):319–330.

Chen, C. C., Tsai, T. H., Huang, Z. R., Fang, J. Y. 2010. Effects of lipophilic emulsifiers on the oral administration of lovastatin from nanostructured lipid carriers: Physicochemical characterization and pharmacokinetics. European Journal of Pharmaceutics and Biopharmaceutics, 74(3):474–482.

Chen, P., Zhang, H., Cheng, S., Zhai, G., Shen, C. 2016.

Development of curcumin loaded nanostructured lipid carrier based thermosensitive in situ gel for dermal delivery. Colloids and Surfaces A: Physicochemical and Engineering Aspects, 506:356–362.

Chen-Yu, G., Chun-Fen, Y., Qi-Lu, L., Qi, T., Yan-Wei, X., Wei-Na, L., Guang-Xi, Z. 2012. Development of a Quercetin-loaded nanostructured lipid carrier formulation for topical delivery. International Journal of Pharmaceutics, 430(1-2):292–298.

Chien, M. H., Ying, T. H., Hsieh, Y. S., Chang, Y. C., Yeh, C. M., Ko, J. L., Yang, S. F. 2012. Dioscorea nipponica Makino inhibits migration and invasion of human oral cancer HSC-3 cells by transcriptional inhibition of matrix metalloproteinase-2 through modulation of CREB and AP-1 activity. Food and Chemical Toxicology, 50(3-4):558–566.

Cho, Y. J., Zhang, B., Kaartinen, V., Haataja, L., Curtis, I. D., Groffen, J., Heisterkamp, N. 2005. Generation of rac3 Null Mutant Mice: Role of Rac3 in Bcr/Abl-Caused Lymphoblastic Leukemia. Molecular and Cellular Biology, 25(13):5777–5785.

Doktorovova, S., Souto, E. B. 2009. Nanostructured lipid carrier-based hydrogel formulations for drug delivery: A comprehensive review. Expert Opinion on Drug Delivery, 6(2):165–176.

Fahmy, U. A., Aljaeid, B. M. 2016. Combined strategy for suppressing breast carcinoma MCF-7 cell lines by loading simvastatin on alpha lipoic acid nanoparticles. Expert Opinion on Drug Delivery, 13(12):1653–1660.

Fujiwara, K., Tsubaki, M., Yamazoe, Y., Nishiura, S., Kawaguchi, T., Ogaki, M., Nishida, S. 2008. Fluvastatin Induces Apoptosis on Human Tongue Carcinoma Cell Line HSC-3. Yakugaku zasshi, 128(1):153–158.

Gabal, Y. M., Kamel, A. O., Sammour, O. A., Elshafeey, A. H. 2014. Effect of surface charge on the brain delivery of nanostructured lipid carriers in situ gels via the nasal route. International Journal of Pharmaceutics, 473(1-2):442–457.

Han, S. S., Chung, S. T., Robertson, D. A., Ranjan, D., Bondada, S. 1999. Curcumin Causes the Growth Arrest and Apoptosis of B Cell Lymphoma by Downregulation of egr-1, C-myc, Bcl-XL, NF-κB, and p53. Clinical Immunology, 93(2):152–161.

Hirano, M., Matsuoka, H., Kuroiwa, Y., Sato, K., Tanaka, S., Yoshida, T. 1992. Dysphagia following Various Degrees of Surgical Resection for Oral Cancer. Rhinology & Laryngology, 101(2):138–141. Annals of Otology.

Hooff, G. P., Peters, I., Wood, W. G., Müller, W. E., Eckert, G. P. 2010. Modulation of Cholesterol, Farnesylpyrophosphate, and Geranylgeranylpyrophosphate in Neuroblastoma SH-SY5Y-APP695 Cells: Impact on Amyloid Beta-Protein Production. Molecular Neurobiology, 41(2-3):341–350.

Huang, M. T., Lou, Y. R., Ma, W., Newmark, H. L., Reuhl, K. R., Conney, A. H. 1994. Inhibitory Effects of Dietary Curcumin on Forestomach, Duodenal, and Colon Carcinogenesis in Mice. Cancer Research, 54(22):5841–5847.

Ip, S. W., Wu, S. Y., Yu, C. C., Kuo, C. L., Yu, C. S., Yang, J. S., Chung, J. G. 2011. Induction of apoptotic death by curcumin in human tongue squamous cell carcinoma SCC-4 cells is mediated through endoplasmic reticulum stress and mitochondria-dependent pathways. Cell Biochemistry and Function, 29(8):641–650.

Ito, T., Yeo, Y., Highley, C. B., Bellas, E., Benitez, C. A., Kohane, D. S. 2007. The prevention of peritoneal adhesions by in situ cross-linking hydrogels of hyaluronic acid and cellulose derivatives. Biomaterials, 28(6):975–983.

Jabarian, L. E., Rouini, M. R., Atyabi, F., Foroumadi, A., Nassiri, S. M., Dinarvand, R. 2013. In vitro and in vivo evaluation of an in situ gel forming system for the delivery of PEGylated octreotide. European Journal of Pharmaceutical Sciences, 48(1-2):87–96.

Jayaprakasha, G. K., Rao, L., Sakariah, K. K. 2006. Antioxidant activities of curcumin, demethoxycurcumin and bisdemethoxycurcumin. Food Chemistry, 98(4):720–724.

Jeong, B., Bae, Y. H., Kim, S. W. 2000. In situ gelation of PEG-PLGA-PEG triblock copolymer aqueous solutions and degradation thereof. Journal of Biomedical Materials Research, 50(2):171–177.

Lin, C. C. 2007. Berberine induces apoptosis in human HSC-3 oral cancer cells via simultaneous activation of the death receptor-mediated and mitochondrial pathway. Anticancer research, 27(5A):3371–3378.

Madane, R. G., Mahajan, H. S. 2016. Curcumin-loaded nanostructured lipid carriers (NLCs) for nasal administration: design, characterization, and in vivo study. Drug Delivery, 23(4):1326–1334.

Masuda, T., Hidaka, K., Shinohara, A., Maekawa, T., Takeda, Y., Yamaguchi, H. 1999. Chemical Studies on Antioxidant Mechanism of Curcuminoid: Analysis of Radical Reaction Products from Curcumin. Journal of Agricultural and Food Chemistry, 47(1):71–77.

Nakashima, A., Saxer, C., Niina, M., Masuda, N., Iwasaki, K., Furukawa, K. 2001. Determination of fluvastatin and its five metabolites in human plasma using simple gradient reversed-phase

high-performance liquid chromatography with ultraviolet detection. Journal of Chromatography B: Biomedical Sciences and Applications, 760(1):17–25.

Radtke, M., Müller, R. H. 2001. Nanostructured lipid drug carriers. New Drugs, 2:48–52.

Rashmi, R. 2004. Ectopic expression of Bcl-XL or Ku70 protects human colon cancer cells (SW480) against curcumin-induced apoptosis while their down-regulation potentiates it. Carcinogenesis, 25(10):1867–1877.

Ruel-Gariépy, E., Leroux, J. C. 2004. In situ-forming hydrogels-review of temperature-sensitive systems. European Journal of Pharmaceutics and Biopharmaceutics, 58(2):409–426.

Sun, M., Estrov, Z., Ji, Y., Coombes, K. R., Harris, D. H., Kurzrock, R. 2008. Curcumin (diferuloylmethane) alters the expression profiles of microRNAs in human pancreatic cancer cells. Molecular Cancer Therapeutics, 7(3):464–473.

Taheri, A., Atyabi, F., Dinarvnd, R. 2011. Temperature-responsive and biodegradable PVA:PVP k30:poloxamer 407 hydrogel for controlled delivery of human growth hormone (hGH). Journal of Pediatric Endocrinology and Metabolism, 24(3-4):175–179. Retrieved.

Taylor, F., Ebrahim, S., *et al.* 2011. Statins for the primary prevention of cardiovascular disease. Cochrane Database of Systematic Reviews, (1).

Teeranachaideekul, V., Muller, R., Junyaprasert, V. 2007. Encapsulation of ascorbyl palmitate in nanostructured lipid carriers (NLC)-Effects of formulation parameters on physicochemical stability. International Journal of Pharmaceutics, 340(1-2):198–206.

Tricarico, P., Crovella, S., Celsi, F. 2015. Mevalonate Pathway Blockade, Mitochondrial Dysfunction and Autophagy: A Possible Link. International Journal of Molecular Sciences, 16(7):16067–16084.

Uner, M. 2006. Preparation, characterization and physico-chemical properties of solid lipid nanoparticles (SLN) and nanostructured lipid carriers (NLC): their benefits as colloidal drug carrier systems. Die Pharmazie, (5):375–386.

Visvikis, O., Lorès, P., Boyer, L., Chardin, P., Lemichez, E., Gacon, G. 2008. Activated Rac1, but not the tumorigenic variant Rac1b, is ubiquitinated on Lys 147 through a JNK-regulated process. FEBS Journal, 275(2):386–396.

Warnakulasuriya, S. 2009. Global epidemiology of oral and oropharyngeal cancer. Oral Oncology, 45(4-5):309–316.

Wheeler, A. P. 2006. Rac1 and Rac2 regulate macrophage morphology but are not essential for migration. Journal of Cell Science, 119(13):2749–2757.

Yuan, L., Zhang, Z., Wei, C., Zhou, L., Wu, Q., Chen, Y. 2012. Effect of cell-penetrating peptide-coated nanostructured lipid carriers on the oral absorption of tripterine. International Journal of Nanomedicine, 4581.

Zhang, L. 2002. Development and in-vitro evaluation of sustained release Poloxamer 407 (P407) gel formulations of ceftiofur. Journal of Controlled Release, 85(1-3):73–81.

Zhang, X., Liu, J., Qiao, H., Liu, H., Ni, J., Zhang, W., Shi, Y. 2010. Formulation optimization of dihydroartemisinin nanostructured lipid carrier using response surface methodology. Powder Technology, 197(1-2):120–128.

Zhou, L. 2012. Preparation of tripterine nanostructured lipid carriers and their absorption in rat intestine. Die Pharmazie-An International Journal of Pharmaceutical Sciences, 67(4):304–310. Avoxa-Mediengruppe Deutscher Apotheker GmbH.